JYX
JYVÄSKYLÄN YLIOPISTO
UNIVERSITY OF JYVÄSKYLÄ

This is a self-archived version of an original article. This version may differ from the original in pagination and typographic details.

Author(s): Csókás, Dániel; Siitonen, Juha H.; Pihko, Petri M.; Pápai, Imre

Title: Conformationally Locked Pyramidality Explains the Diastereoselectivity in the Methylation of trans-Fused Butyrolactones

Year: 2020

Version: Published version

Copyright: © 2020 American Chemical Society

Rights: CC BY 4.0

Rights url: https://creativecommons.org/licenses/by/4.0/

Please cite the original version:

Csókás, D., Siitonen, J. H., Pihko, P. M., & Pápai, I. (2020). Conformationally Locked Pyramidality Explains the Diastereoselectivity in the Methylation of trans-Fused Butyrolactones. Organic Letters, 22(12), 4597-4601. https://doi.org/10.1021/acs.orglett.0c01008

This is an open access article published under a Creative Commons Attribution (CC-BY) License, which permits unrestricted use, distribution and reproduction in any medium, provided the author and source are cited.

ACS AUTHORCHOICE

OL | Organic Letters

pubs.acs.org/OrgLett

Letter

Conformationally Locked Pyramidality Explains the Diastereoselectivity in the Methylation of *trans*-Fused Butyrolactones

Dániel Csókás, Juha H. Siitonen, Petri M. Pihko,* and Imre Pápai*

Cite This: *Org. Lett.* 2020, 22, 4597−4601

Read Online

ACCESS | Metrics & More | Article Recommendations | Supporting Information

ABSTRACT: A stereoselectivity model inspired by the total synthesis of stemona alkaloids is developed to explain why enolate-derived 3,4-fused butyrolactones are methylated with a preference for *syn* alkylation. The model shows how conformational locking present in nonplanar enolate structures favors *syn* over *anti* methylation, due to less significant structural distortions in the *syn* pathway. The developed model was also successfully used to rationalize selectivities of previously documented methylation reactions.

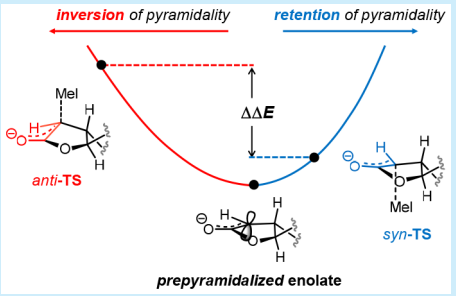

During our work on the total synthesis of stemoamides, we discovered a marked preference for the methylation of the enolate derived from 9a-*epi*-norstemoamide **1** to give a *syn* product **2** (Figure 1a).[1] The same sense of selectivity has been reported on several occasions for a range of *trans*-fused γ-butyrolactones,[2] but the observed selectivity has not been explained in the literature (for selected lactones, see **3**−**5** in Figure 1a). Typically, enolate face selectivity has been rationalized on the basis of either steric effects alone or through a combination of steric and stereoelectronic effects.[3] The *trans*-fused lactones of Figure 1a, however, do not appear to have any obvious steric bias, and there are no obvious stereoelectronic effects that would readily explain the observed selectivity. Torsional effects have been found to be of key importance in stereoselective electrophilic addition reactions,[4] including alkylations of various five-membered ring enolates.[5] However, to invoke torsional effects as an explanation requires a full computational analysis of the relevant transition states (TSs), and as such, these TS-based arguments may remain less accessible to a synthetic chemist in planning a stereoselective synthesis.

Herein, we present a detailed computational analysis of the stereocontrol elements in methylation reactions of 3,4-*trans*-fused butyrolactones. We demonstrate that the stereoselectivity of the methylation of this class of butyrolactones can simply be deduced from the sense of pyramidality of the ground state (GS) of the enolate, which is constrained by the ring fusion.[6] The pyramidality can be quantified by the O−C−C−H torsion angle ϕ. We predict that the *syn* attack is favored because it involves a smaller change of ϕ and thereby a smaller distortion in the TS compared with the *anti* attack.

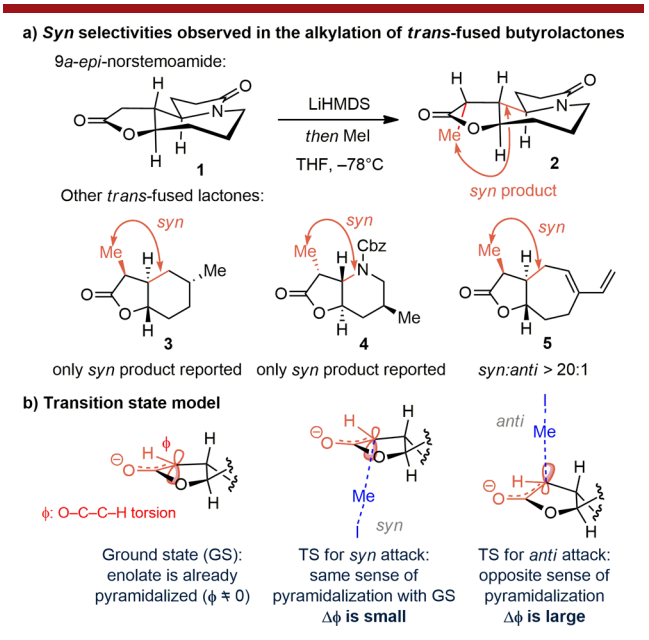

Figure 1. Selected experimental observations (a) and the proposed stereoselectivity model (b).

Received: March 19, 2020
Published: April 27, 2020

Downloaded via UNIV OF JYVASKYLA on June 23, 2020 at 05:10:52 (UTC).
See https://pubs.acs.org/sharingguidelines for options on how to legitimately share published articles.

For 9a-*epi*-norstemoamide, DFT calculations pointed to a slight thermodynamic preference for the *anti*-methylated product; however, the formation of the *syn* product was found to be kinetically favored.[1] No steric effects could be identified in the located transition states, and we hypothesized that the preferential *syn* attack of the methylating agent is associated with the prepyramidalization of the nucleophilic carbon atom of the enolate (Figure 1b), potentially providing a less strained transition state for *syn* methylation.

In our computational analysis, we first employed the energy decomposition scheme offered by the activation strain model (ASM)[7] to the transition states identified for the *syn* and *anti* methylation pathways of 9a-*epi*-norstemoamide (see ***syn*-TS** and ***anti*-TS** in Figure 2). The relatively early nature of these

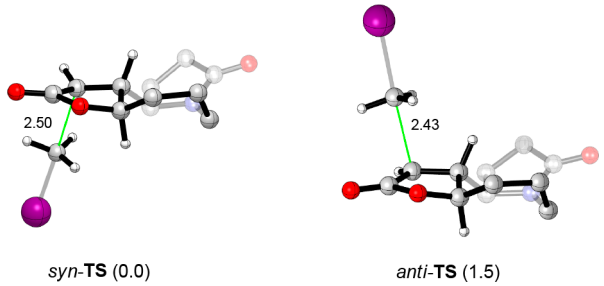

Figure 2. Transition states computed for the *syn* and *anti* methylation pathways of 9a-*epi*-norstemoamide **1**. Relative stabilities ($\Delta\Delta G$) are given in parentheses (in kcal/mol), forming C···C distances in Å. H atoms of the enolate (except those of the butyrolactone ring) are omitted for clarity.

transition states (the reacting carbon atoms are at least 2.4 Å apart in these transition states) justifies the relevance of this approach,[8] which has been widely applied to rationalize reactivities and selectivities.[7,9]

The energy components obtained from the ASM analysis are listed in Table 1, and the results reveal that the difference in the electronic energies of the two diastereomeric transition states ($\Delta\Delta E^{\ddagger}$ = 2.1 kcal/mol) is predominantly related to the distortion (i.e., structural change) of the reactants (enolate **en** and MeI) with respect to their ground-state structures. The

Table 1. Energy Data from ASM Analysis (in kcal/mol)[a]

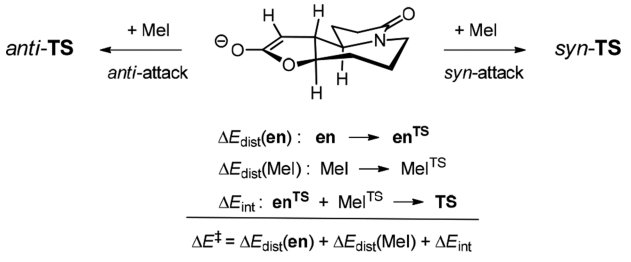

energy component	*anti*-TS	*syn*-TS	$\Delta\Delta E$[b]
ΔE_{dist}(**en**)	2.9	1.0	1.9
ΔE_{dist}(MeI)	12.9	11.8	1.1
ΔE_{int}	−19.5	−18.6	−0.9
$\Delta E^{\ddagger}$	−3.7	−5.8	2.1

[a]Energy data are obtained form electronic energies computed at the ωB97X-D/Def2TZVPP level. **en**^{TS} and MeI^{TS} denote distorted structures of the reactants in the transition states. [b]Energy difference obtained from the previous two columns.

distortion of the reacting partners involves the elongation of the Me−I bond and significant pyramidalization of the enolate C_{10} carbon atom required for C−C bond formation.[1] The distortion energies ΔE_{dist}(**en**) and ΔE_{dist}(MeI) are notably higher in the disfavored transition state ***anti*-TS** as compared to ***syn*-TS**, although the overall effect ($\Delta\Delta E_{dist}$(**en**) + $\Delta\Delta E_{dist}$(MeI) = 3.0 kcal/mol) is somewhat reduced when considering the difference in the interaction energies ($\Delta\Delta E_{int}$ = −0.9 kcal/mol). Altogether, the total energy difference ($\Delta\Delta E^{\ddagger}$ = 2.1 kcal/mol) is well captured by the distortion energies of the enolate ($\Delta\Delta E_{dist}$(**en**) = 1.9 kcal/mol).[10]

The ASM analysis thus implies increased distortion (strain) in the enolate along the *anti* alkylation pathway, which is also apparent from the torsion angles associated with the forming C−C bond. As illustrated in Figure 3, the vicinal bonds

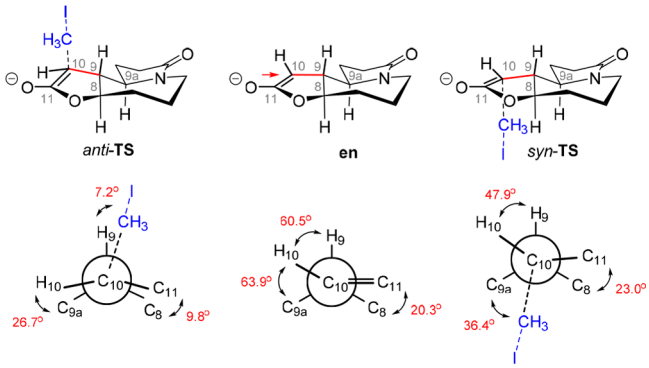

Figure 3. Dihedral angles relevant to torsional strain in enolate **en** and in the transition states of methylation. Newman projections are viewed from the direction indicated by the red arrow.

adjacent to the reacting C_{10} carbon atom are fairly close to the eclipsed arrangement in the ***anti*-TS**, whereas no such small torsion angles are seen in the more favored ***syn*-TS** or in the ground-state enolate **en**. It thus appears that the concept of torsional control of stereoselectivity[4] can be applied for the present reaction as well.

To assess the relation between the torsional strain induced in the enolate along the two methylation pathways and the degree of pyramidalization of the enolate C_{10} carbon atom, we examined the energy variation of the bare enolate **en** (i.e., without MeI) as a function of the O−C═C−H dihedral angle (see Figure 4). This torsion angle ϕ is a natural choice to quantify the deviation from the planar enolate structure and the pyramidality of the C_{10} atom. Computations predict ϕ = 12.6° for the ground-state structure of enolate **en**. The potential energy curve depicted in Figure 4 indicates that the energy penalty of reaching the dihedral angle measured in the ***anti*-TS** transition state (ϕ = −22.1°) via the inversion of pyramidality is 1.8 kcal/mol larger than the energy change accompanied by the pyramidalization at ***syn*-TS** (ϕ = 25.6°). This energy difference is almost identical to that obtained in the strain analysis for the distortion of the enolate ($\Delta\Delta E_{dist}$(**en**) = 1.9 kcal/mol), suggesting that the dihedral angle ϕ is a reasonable indicator of the torsional strain induced on the two methylation pathways.

The role of ring fusion and pyramidality in stereoselectivity control was evaluated next by carrying out DFT calculations for selected model enolates (Figure 5a).[11] The simple γ-butyrolactone enolate $\mathbf{en}_{but}$ exhibits a nonplanar equilibrium structure with a pyramidalized carbon center (ϕ = 9.6°). The

https://dx.doi.org/10.1021/acs.orglett.0c01008
Org. Lett. 2020, 22, 4597−4601

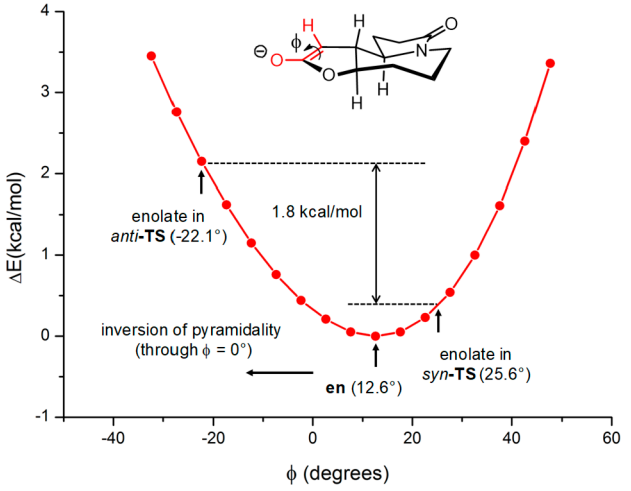

Figure 4. Potential energy curve derived by constrained geometry optimization of enolate **en** varying the O−C−C−H dihedral angle (highlighted in red). Dihedral angles measured in the optimized structures of **en** and the two transition states are marked by arrows.

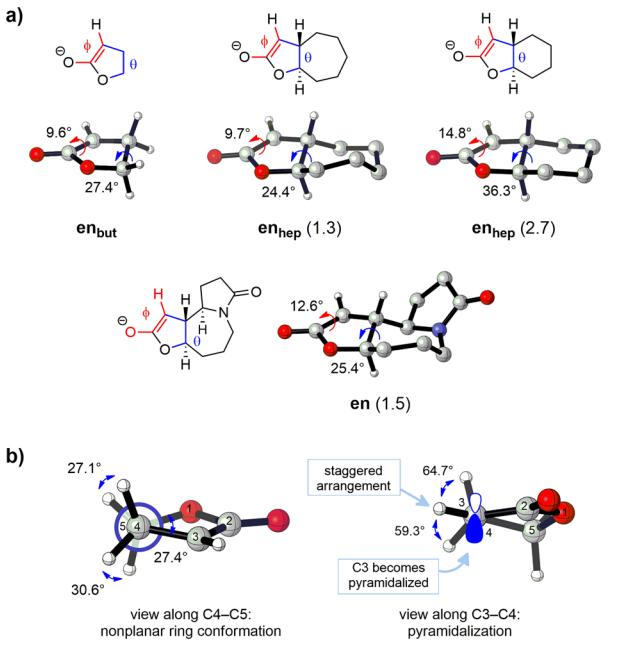

Figure 5. (a) Selected model enolates with characteristic torsion angles (ϕ and θ; as defined by the O−C=C−H and O−C−C−C units of the cyclic enolates). Data obtained for enolate **en** are also given for reference. Computed stereoselectivities ($\Delta\Delta G$ data; in kcal/mol) are given in parentheses. Most of the hydrogen atoms (except those of the butyrolactone ring) are omitted for clarity. (b) Rationalization of the sense of pyramidalization, using enolate $\mathbf{en}_{but}$ as an example.

pyramidalization arises from minimization of torsional strain of the five-membered ring. The C4−C5 bond adopts a non-eclipsed conformation (Figure 5b, left), and the resulting nonplanar ring (twist, $^4T_5$ conformation) is further stabilized by pyramidalization at C3 as the C3−H bond adopts a staggered arrangement with the vicinal C4−H bonds (Figure 5b, right).

Interestingly, *trans*-fusion with a cycloheptane ring does not alter the pyramidality of the nucleophilic carbon atom ($\mathbf{en}_{hep}$; ϕ = 9.7°); however, a more constrained cyclohexane ring exhibits increased pyramidality ($\mathbf{en}_{hex}$; ϕ = 14.8°). The pyramidality of the C_{10} carbon atom in enolate **en** is somewhat between those in $\mathbf{en}_{hep}$ and $\mathbf{en}_{hex}$, implying that the azepane ring and the cyclic amide unit in the *trans*-fused system impose additional structural restraint in the enolate. The dihedral angle defined by the O−C−C−C unit of the five-membered ring (θ in Figure 5a) represents another characteristic structural parameter of the cyclic enolates, and they also point to an enhanced distortion effect in $\mathbf{en}_{hex}$. Transition states for the *syn* and *anti* methylation pathways for bicyclic enolates $\mathbf{en}_{hep}$ and $\mathbf{en}_{hex}$ were computed, and the predicted selectivities (see $\Delta\Delta G$ values in Figure 5a) correlate fairly well with the ϕ dihedral angle.[12]

We note that the ground-state structure of enolate $\mathbf{en}_{but}$ is flexible because the nonplanar five-membered ring can easily flip. The ring inversion occurs via a planar transition structure, so it involves the variation of the θ dihedral angle as well (see Figure 6). The rotational flexibility is restricted in fused

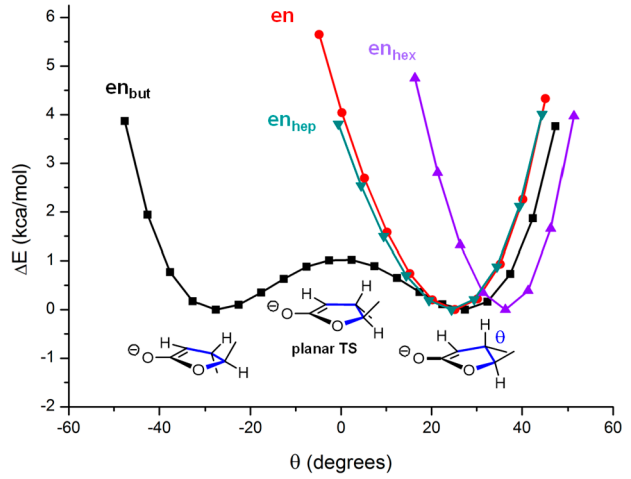

Figure 6. Potential energy curves derived by constrained geometry optimization of various enolates varying the θ dihedral angle.

bicyclic enolates. This is apparent from the $\Delta E(\theta)$ potential energy curves computed for *trans*-fused enolates **en**, $\mathbf{en}_{hep}$, and $\mathbf{en}_{hex}$, which all display a single energy minimum, and a substantial amount of energy is required to reach the planar (θ = 0°) region. Consequently, the nonplanar conformations of these enolates are confined (locked), and the innate pyramidality of the nucleophilic carbon provides an energetic bias for the *syn* methylation pathway as discussed above.

We have also examined a number of methylation reactions reported for bi- and tricyclic *trans*-fused butyrolactones,[2] and our DFT calculations confirm the *syn* selectivity observed in all these cases (Figure 7).[13] For the complex 5 + 7 + 5 tricyclic fused systems **A**[2a] and **B**,[2b] we find a similar degree of selectivities as for our target reaction with 9a-*epi*-norstemoamide **1**. The *syn* selectivity increases slightly when unsaturation is introduced in the seven-membered ring (product **C**).[2c−e] In accordance with the results obtained for model $\mathbf{en}_{hex}$, calculations predict further enhanced selectivities for all 5 + 6 bicyclic systems (**D**−**H**),[2f−k] which are particularly high if heteroatoms are involved in the six-membered ring (**G** and **H**).[2j,k] In these latter cases, the bicyclic systems bear bulky substituents as well (OBn and Cbz), but no steric effects could be identified that would alter the selectivity.

https://dx.doi.org/10.1021/acs.orglett.0c01008
Org. Lett. 2020, 22, 4597−4601

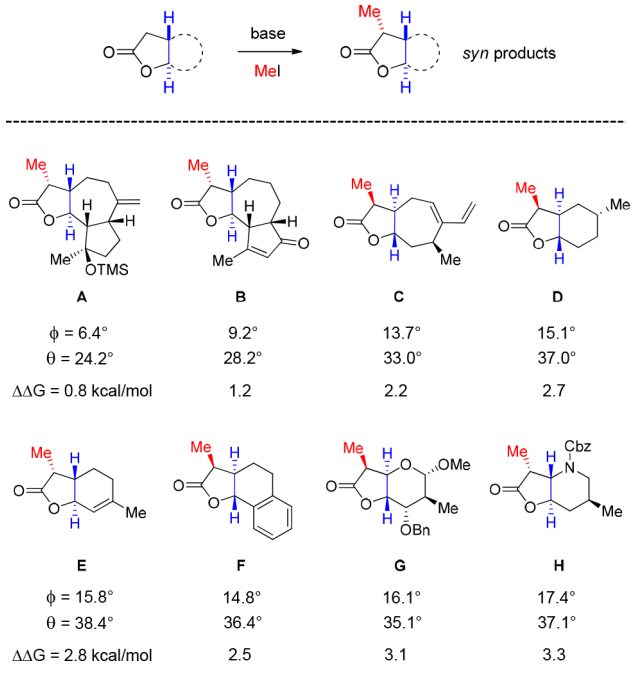

Figure 7. *Syn* products observed in various alkylation processes and selected computed properties (ϕ and θ as torsion angles of corresponding enolates; $\Delta\Delta G$ as predicted selectivities).

In summary, we have disclosed how methylation of 3,4-*trans*-fused butyrolactones occurs in a *syn*-selective fashion. The nucleophilic carbon center of the five-membered ring enolate is pyramidalized. The direction of the pyramidalization is essentially determined by the stereochemistry of the *trans*-ring fusion. The nonplanar enolate structure prefers alkylation from the direction of the pyramidalization, affording a kinetically more favored pathway for the formation of *syn* products. The emerging model implies that the stereoselectivity of this class of methylation reactions can be inferred simply from the ground-state structure of the enolate, i.e., without the inspection of the diastereomeric methylation transition states. The results obtained herein are a testimony to how total synthesis efforts can help to identify gaps in both synthetic methodology as well as in our understanding of stereoselectivity.

■ ASSOCIATED CONTENT

Supporting Information

The Supporting Information is available free of charge at https://pubs.acs.org/doi/10.1021/acs.orglett.0c01008.

Computational details, optimized structures, total energy components, and Cartesian coordinates (PDF)

■ AUTHOR INFORMATION

Corresponding Authors

Imre Pápai − *Institute of Organic Chemistry, Research Centre for Natural Sciences, H-1117 Budapest, Hungary;* orcid.org/0000-0002-4978-0365; Email: papai.imre@ttk.mta.hu

Petri M. Pihko − *Department of Chemistry, Nanoscience Centre, University of Jyväskylä, FI-40014 Jyväskylä, Finland;* orcid.org/0000-0003-0126-0974; Email: petri.pihko@jyu.fi

Authors

Dániel Csókás − *Institute of Organic Chemistry, Research Centre for Natural Sciences, H-1117 Budapest, Hungary;* orcid.org/0000-0002-4150-477X

Juha H. Siitonen − *Department of Chemistry, Nanoscience Centre, University of Jyväskylä, FI-40014 Jyväskylä, Finland;* orcid.org/0000-0002-9816-637X

Complete contact information is available at: https://pubs.acs.org/10.1021/acs.orglett.0c01008

Author Contributions

The manuscript was written through contributions of all authors. All authors have given approval to the final version of the manuscript.

Notes

The authors declare no competing financial interest.

■ ACKNOWLEDGMENTS

Financial support from the Academy of Finland (project #259532), Jenny and Artturi Wihuri Foundation (research grant to J.H.S.), University of Jyväskylä (postgraduate fellowship to J.H.S), and NKFIH Hungary (grant K-112028) is gratefully acknowledged. We thank T. Földes and Á. Madarász for helpful discussions and practical advice.

■ REFERENCES

(1) Siitonen, J. H.; Csókás, D.; Pápai, I.; Pihko, P. M., submitted for publication.

(2) (a) Devreese, A. A.; De Clercq, P. J.; Vandewalle, M. *Tetrahedron Lett.* **1980**, *21*, 4767−4770. (b) Lee, E.; Yoon, C. H.; Sung, Y.-s.; Kim, Y. K.; Yun, M.; Kim, S. *J. Am. Chem. Soc.* **1997**, *119*, 8391−8392. (c) Evans, M. A.; Morken, J. P. *Org. Lett.* **2005**, *7*, 3371−3373. (d) Matsumoto, K.; Koyachi, K.; Shindo, M. *Tetrahedron* **2013**, *69*, 1043−1049. (e) Matsuo, K.; Yokoe, H.; Shishido, K.; Shindo, M. *Tetrahedron Lett.* **2008**, *49*, 4279−4281. (f) Forzato, C.; Nitti, P.; Pitacco, G.; Valentin, E. *Gazz. Chim. Ital.* **1996**, *126*, 37−44. (g) Jung, M. E.; Im, G. Y. J. *Tetrahedron Lett.* **2008**, *49*, 4962−4964. (h) Jung, M. E.; Im, G-Y. J. *J. Org. Chem.* **2009**, *74*, 8739−8753. (i) Suzuki, K.; Tatsuoka, T.; Ishihara, T.; Ohno, T.; Aisaka, K.; Ogino, R.; Kuroki, M.; Satoh, F.; Miyano, S.; Sumoto, K. *Chem. Pharm. Bull.* **1996**, *44*, 132−138. (j) Sasaki, M.; Inoue, M.; Takamatsu, K.; Tachibana, K. *J. Org. Chem.* **1999**, *64*, 9399−9415. (k) Taber, D. F.; DeMatteo, P. W. *J. Org. Chem.* **2012**, *77*, 4235−4241.

(3) For comprehensive reviews, see: (a) Evans, D. A. Stereoselective Alkylation of Chiral Metal Enolates. In *Asymmetric Synthesis*; Morrison, J. D., Ed.; Academic Press, 1984; Vol. 3. (b) Caine, D. Alkylations of Enols and Enolates. In *Comprehensive Organic Synthesis*; Trost, B. M., Fleming, I., Eds.; Pergamon Press: Oxford, 1991; Vol. 3, ch. 1.1. (c) Carreira, E. M.; Kvaerno, L. *Classics in Stereoselective Synthesis*; Wiley-VCH: Weinheim, 2009; ch. 3, p 73. (d) Stoltz, B. M.; Bennett, N. B.; Duquette, D. C.; Goldberg, A. F. G.; Liu, Y.; Loewinger, M. B.; Reeves, C. M. Alkylation of Enols and Enolates. In *Comprehensive Organic Synthesis*; Knochel, P., Molander, G., Eds.; 2014; Vol. 3, ch. 3.01.

(4) Wang, H.; Houk, K. N. *Chem. Sci.* **2014**, *5*, 462−470.

(5) For relevant studies, see: (a) Meyers, A. I.; Seefeld, M. A.; Lefker, B. A.; Blake, J. F. *J. Am. Chem. Soc.* **1997**, *119*, 4565−4566. (b) Ando, K.; Green, N. S.; Li, Y.; Houk, K. N. *J. Am. Chem. Soc.* **1999**, *121*, 5334−5335. (c) Ando, K. *J. Am. Chem. Soc.* **2005**, *127*, 3964−3972. (d) Soteras, I.; Lozano, O.; Gómez-Esqué, A.; Escolano, C.; Orozco, M.; Amat, M.; Bosch, J.; Luque, F. J. *J. Am. Chem. Soc.* **2006**, *128*, 6581−6588. (e) Jiménez-Osés, G.; Aydillo, C.; Busto, J. H.; Zurbano, M. M.; Peregrina, J. M.; Avenoza, A. *J. Org. Chem.* **2007**, *72*, 5399−5402. (f) Aydillo, C.; Jiménez-Osés, G.; Busto, J. H.; Peregrina, J. M.; Zurbano, M. M.; Avenoza, A. *Chem. - Eur. J.* **2007**,

13, 4840−4848. (g) Hsu, D. C.; Lam, P. C.-H.; Slebodnick, C.; Carlier, P. R. *J. Am. Chem. Soc.* **2009**, *131*, 18168−18176. (h) Volp, K. A.; Harned, A. M. *J. Org. Chem.* **2013**, *78*, 7554−7564. (i) Harned, A. M. *Chem. Commun.* **2015**, *51*, 2076−2079. (j) Gutiérrez-Jiménez, M. I.; Aydillo, C.; Navo, C. D.; Avenoza, A.; Corzana, F.; Jiménez-Osés, G.; Zurbano, M. M.; Busto, J. H.; Peregrina, J. M. *Org. Lett.* **2016**, *18*, 2796−2799. (k) Moon, N. G.; Harned, A. M. *Org. Biomol. Chem.* **2017**, *15*, 1876−1888.

(6) Correlation between the pyramidalization of trigonal carbon centers and the stereoselectivity of addition reactions has long been recognized. For seminal works, see: (a) Rondan, N. G.; Paddon-Row, M. N.; Caramella, P.; Houk, K. N. *J. Am. Chem. Soc.* **1981**, *103*, 2436−2438. (b) Seebach, D.; Maetzke, T.; Petter, W.; Klötzer, B.; Plattner, D. A. *J. Am. Chem. Soc.* **1991**, *113*, 1781−1786 and references therein..

(7) Bickelhaupt, F. M.; Houk, K. N. *Angew. Chem., Int. Ed.* **2017**, *56*, 10070−10086.

(8) The ASM analysis is a fragment-based approach that relies on the properties of reactants (distortion and interaction), so it assumes relatively early transition states.

(9) Fernández, I.; Bickelhaupt, F. M. *Chem. Soc. Rev.* **2014**, *43*, 4953−4967.

(10) For details of ASM analysis, see the Supporting Information.

(11) For optimal structures and relative stabilities, see the Supporting Information.

(12) For the analysis of torsional strain in this series of enolates in terms of $\Delta E(\phi)$ potential energy curves, see the Supporting Information.

(13) For computed transition states and relative stabilities, see the Supporting Information.

https://dx.doi.org/10.1021/acs.orglett.0c01008
Org. Lett. 2020, 22, 4597−4601